Title

THE PROPERTIES OF THE NON-SPECULAR LOW ENERGY ELECTRON DIFFRACTION BEAMS SCATTERED BY THE (100) FACE OF FACE CENTERED CUBIC METAL SINGLE CRYSTALS

Permalink

https://escholarship.org/uc/item/5619p0mx

Authors

Farrell, H.H.
Somorjai, G.A.

Publication Date

1969-03-01

THE PROPERTIES OF THE NON-SPECULAR LOW ENERGY ELECTRON DIFFRACTION BEAMS SCATTERED BY THE (100) FACE OF FACE CENTERED CUBIC METAL SINGLE CRYSTALS

H. H. Farrell and G. A. Somorjai

March 1969

LAWRENCE RADIATION LABORATORY
UNIVERSITY of CALIFORNIA BERKELEY

DISCLAIMER

The Properties of the Non-Specular

Low Energy Electron Diffraction Beams Scattered

By the (100) Face of Face Centered

Cubic Metal Single Crystals

H. H. Farrell and G. A. Somorjai

Inorganic Materials Research Division, Lawrence Radiation Laboratory,
Department of Chemistry,
University of California, Berkeley, California

Abstract

The intensities of the non-specular low energy electron beams

diffracted from the Al(100) and Pd(100) surfaces were measured as a

function of electron energy in the range 5-200 eV at room temperature.

The experimental results were correlated with $I_{h,k}$-eV curves which

were obtained from Ni(100), Cu(100), Ag(100) and Au(100) surfaces.

Single and double diffraction conditions were adequate to compute the

positions of most of the maxima. The double diffraction condition,

$2\vec{K}_z = \vec{G}_z$, appears to be especially important at low electron energies.

The intensities and shape of the diffraction peaks are strongly

influenced by the atomic potential.

Introduction

Experimental low energy electron diffraction studies of metal surfaces have a long history which begins with the Davisson-Germer[1] experiment in 1927. However, unlike the case of X-ray diffraction, theoretical interpretations of the diffraction feature have been incomplete or only partially satisfactory, particularly in the very low energy (less than approximately (100 eV) region. The relatively large values of atomic scattering cross sections for low energy electron diffraction (LEED) necessitate the consideration of multiple scattering phenomena. Recently, E. G. McRae[2] has developed a formally complete and self-consistent theory of dynamical low energy electron diffraction. In the subsequent months, there have been a large number of theoretical papers[3,4,5,6] and calculations[7,8] published which all point out the importance of multiple scattering in analyzing the intensities of the diffraction spots to obtain information about the arrangement of atoms in the surface. Concurrently there is a great demand for complete and suitable experimental data to compare with computational results.[8] The importance of multiple scattering in low energy electron diffraction has been experimentally verified by the observation of two phenomena, a) surface wave resonance and b) the appearance of "secondary" diffraction peaks in the I_{hk} - eV curves. Surface wave resonance accompanies the emergence of new diffraction beams. Perhaps the most dramatic manifestation of this effect occurs when a defocussed specularly reflected beam is monitored at a voltage where a diffracted beam should emerge from the crystal. An easily detectable minimum occurs in the intensity of the

observed diffraction spot.[9] Perhaps more significant verification has also
resulted from the observation of "secondary" or fractional order,
Bragg peaks in the specularly reflected electron beam when its intensity
is monitored as a function of electron energy $[I_{00}$ vs. eV].[9,10] Much of
the emphasis up to this time has been placed on the theoretical interpreta-
tion of the characteristics of this specularly reflected electron beam
(the (00) beam).

A great deal of information could be obtained on the nature of low
energy electron diffraction from the properties of the non-specular
electron beams. There is already a wealth of experimental data in the
literature on these diffracted beams. It is the purpose of this paper
to present new and detailed experimental data on the characteristics of
non-specular beams from the (100) face of aluminum and palladium surfaces
and to correlate these with existing data on other face centered cubic
metal surfaces. We hope that the experimental data given here will be
applicable to further the development of realistic theoretical calculations.
The interplay between accurate experimental data and theoretical calculations
should lead to structural analysis of metal surfaces.

Experimental

A conventional Varian LEED apparatus of the post-acceleration type[11]
was employed. The back-diffracted electrons were accelerated onto a
phosphor (P4 bluish-white) screen on which the diffraction spots were
displayed. The resulting fluorescent intensity was monitored with a
telephotometer (Gamma Scientific No. 2000 with fiber optics and a

variable aperture $6' \rightarrow 3°$) as a function of beam voltage. It should

be noted that the intensity vs. voltage (I vs. eV) curves were <u>not</u>

normalized to eliminate variations in emission current. In the

electron gun, a Phillips cathode[12] was used. This was found to have

somewhat poorer resolution characteristics (± 5 eV) than the standard

Varian gun. To compensate for this, a third grid was installed

between the standard suppressor grid and the screen, and was operated as an

auxiliary suppressor grid. All measurements were carried out at 10^{-10}-

10^{-9} torr ambient pressures.

Aluminum and palladium samples were prepared from ultra-high

purity single crystals.[13] These crystals were X-ray oriented to within

2° of the (100) face and the samples were then spark cut to around 1 mm

thickness for the palladium and 3 mm for the aluminum. After polishing

and etching, the palladium sample was mounted on tantalum holders. Because

of the relatively higher solid solubility of aluminum in tantalum, to

prevent contamination the aluminum samples were placed in high purity

aluminum boats before mounting on the tantalum holders. On both samples,

ion bombardment and subsequent annealing heat treatments were used to

obtain an ordered surface with sharp diffraction features. Under the

conditions employed, no surface structures were to be expected on aluminum.[14]

Extensive ion bombardments (>36 hours) and high temperature anneals

(>450°C) were used to insure the absence of the amorphous oxide film that

commonly accompanies freshly prepared aluminum surfaces. On palladium,

however, there are several frequently observed surface structures that

are produced by annealing. As these surface structures tend to change

the shape of the I_{hk} vs. eV curves even before a new diffraction pattern

is observable on the screen, we have followed a technique that both we[15]
and Park[16] have employed previously to produce a "normal" (100) surface
on Pd which exhibits a (1 x 1) diffraction pattern. A very light ion
bombardment (2 x 10^{-5} torr argon at 150 eV for 10 minutes) was employed
followed by a short anneal (less than 400°C for 50 minutes) just before
performing the measurements.

Results

    The intensities of several of the low index diffraction beams
as a function of accelerating voltage are shown in Figure 1 for the (100)
face of aluminum, and in Figure 2 for the (100) face of palladium. The
intensities from the non-specularly reflected beams were measured within a degree of
normal incidence (within a degree). As it is impossible to measure the
intensity of the specularly reflected beam, (0,0) beam, at normal incidence
with a post-acceleration apparatus, these intensities were obtained at
an angle of incidence of 3° with respect to the surface normal. It should
be noted that the data is presented as obtained in the experiments. That is,
there have been no corrections made for the current vs. voltage characteristics
of the electron gun (the current increases sharply with increasing beam
voltage) nor for contact potential and other errors in the measured
accelerating potential or for changes in the background intensity. The
measurements were performed at room temperature (25°C). Consequently,
above 150 eV, much of the elastically scattered intensity from aluminum
is obscured by the Debye-Waller effect[17] and multi-phonon processes[18]
which are responsible for most of the background intensity. In Figure 3

we show a schematic diffraction pattern from a (100) surface with the

assignments we have used to identify the diffraction spots. The position

of the diffraction peaks (the electron energy at which the intensity

is at a maximum) from other experiments on (100) faces of several f.c.c.

metals previously reported in the literature[14b,16,19,20,21] are tabulated,

with the data from this laboratory, in Table I. A more detailed comparison

is made for the (1,0) and (1,1) beams from several metals in Figures 4a and

4b. Here, the energy scale has been "normalized" to compensate for

variations in the lattice parameter among the metals [I_{hk} vs. $eVd^2\cos^2\theta$].

As was also found for the specularly reflected (00) beams,[15] the peak

positions for the different materials seem to fall at the same corrected

electron energies when they are plotted on this "normalized" scale.

However, the intensities of these peaks vary considerably from material

to material, presumably reflecting variations in the characteristics

of the atomic potentials. Certain trends have been noted, and will be

discussed in more detail below.

Discussion

A.   Single and Double Diffraction Conditions

The prominent features of low energy electron diffraction are the

result of atomic scattering cross sections that are much larger than

those in X-ray diffraction. In X-ray diffraction, the primary beam

intensity is much larger than the intensity of the scattered beams.

Thus, the probability that an X-ray which is scattered once will be

rescattered again is very small. As a consequence, the only important

diffraction conditions are the classical Bragg conditions which may be

written as

$$\vec{K}' - \vec{K}^\circ = \vec{G} \tag{1}$$

where $\vec{K}^\circ$ is the wave vector of the primary beam, $\vec{K}'$ is the wave vector of a diffracted beam, and $\vec{G}$ is a reciprocal lattice vector. Here, inner potential corrections have been neglected. In low energy electron diffraction, where the cross sections are relatively large, the amplitudes of the various diffracted beams can be of the same order of magnitude as the amplitude of the primary (or incident) beam. As a result, there is a significant probability that an electron may be scattered at least twice before leaving the crystal. Thus, the diffracted beams themselves may behave as "primary" beams or sources of electrons for subsequent scattering events. These double scattering events are characterized by diffraction conditions of the form

$$\vec{K}' - \vec{K}'' = \vec{G} \tag{2}$$

Here, the primes refer to two different diffracted beams. Equation (1) is a special case of this equation. The derivation, and implications of Equation (2) have been extensively discussed by E. G. McRae.[2a] It should be noted that because of these probable multiple scattering events, there may be considerable intensity not only where Equation (1) is met, but also at electron energies and scattering angles where Equation (2) is met. It is one of the features of multiple scattering models that, as observed experimentally for low energy electron diffraction, the intensity vs. energy curves may be more complex than predicted by a single scattering model. Thus, within the double diffraction approximation, to predict the

position of maxima in the I vs. eV curves we must find the electron

energies at which Equation (2) is met. While double diffraction considera-

tions may be employed to predict the position (i.e. energy or wave length)

at which these diffractions are met, higher order multiple scattering

events may contribute to the scattering amplitudes at these positions.

In low energy electron diffraction, the wave vectors of the

diffracted beams are uniquely defined by the energy of the electron,

the lattice periodicity and the experimental geometry. For elastic

scattering, we have the constraint that

$$|\vec{K}^\circ| \;=\; |\vec{K}'| \;=\; \frac{2\pi}{\lambda} \;=\; 2\pi \, (eV/150.4)^{1/2} \tag{3}$$

where $\vec{K}^\circ$ and $\vec{K}'$ are defined above, λ is the wave length of the electron,

and eV is its energy in electron volts. Further, the components of

wave vectors that are parallel to the surface must obey the two-

dimensional diffraction grating formula

$$\vec{K}'_{xy} \;=\; \vec{K}^\circ_{xy} + \vec{G}_{xy} \tag{4}$$

where $\vec{K}'_{xy}$ and $\vec{K}^\circ_{xy}$ are the components of the wave vectors of the

diffracted and the incident beams, respectively, which are parallel to

the surface plane, and $\vec{G}_{xy}$ is a reciprocal lattice vector also parallel

to the surface plane. It may be seen from Equation (4) that Equation (2)

is always obeyed for the parallel components of the wave vectors for all

electron energies and scattering angles. Therefore, we need only

consider under what conditions Equation (2) is met for the components of

the wave vectors that are perpendicular to the surface. Rewriting

Equation (2) for the perpendicular components we have

$$\vec{K}'_z - \vec{K}''_z = \vec{G}_z \qquad\qquad (5)$$

where K'_z and K''_z are the components of the wave vectors of two diffracted

beams which are perpendicular to the surface plane, and $\vec{G}_z$ is some

reciprocal lattice vector which is also perpendicular to the surface.

From the constraints of elastic scattering, and the two-dimensional

grating formula (Equations 3 and 4) the magnitude of the component of the

diffracted beam perpendicular to the surface, $|\vec{K}'_z|$, is uniquely defined as

$$|\vec{K}'_z| = [|\vec{K}^\circ|^2 - |\vec{K}'_{xy}|^2]^{1/2} . \qquad\qquad (6)$$

The perpendicular component, $\vec{K}'_z$, may have both positive and negative

values, corresponding to beams directed into, or out of the crystal.

The advantages of monitoring the intensities of the non-specular

beams at normal electron beam incidence are immediately obvious. Under

these conditions, all of the diffraction beams with the same indices

and the same sign of $\vec{K}'_z$ are degenerate. Consequently, considerably

fewer diffraction conditions of the form given in Equation (5) need be

considered. For example, in the region between approximately 20 and

40 eV, in addition to the transmitted and the specularly reflected beams,

there exist only the first order diffraction beams, four directed into

and four scattered out of the crystal. At normal incidence, the four

beams in these two sets are degenerate. Therefore, there are only

four unique beams in this energy range at normal incidence, and we need only consider three equations of the form of Equation (5). However, away from normal incidence, there may be ten unique beams in this same energy range, and it may be necessary to consider up to forty-five diffraction conditions. The situation becomes increasingly complex as one goes to higher voltage ranges.

Further simplification results from the use of the (100) surface in these studies. The interplanar distances are identical in the two perpendicular directions $a_x \equiv a_x$. Thus the parallel components of the lattice vector are identical $(\vec{G}_x \equiv \vec{G}_y)$.

In Table II we have tabulated the voltages at which Equation (5) is met for the different beams at normal incidence, for scattering from the (100) face of several f.c.c. metals, and in the absence of inner potential corrections. These calculated positions for the intensity maxima may be compared with those observed experimentally. The various observed peaks are tentatively assigned to the different simple and double diffraction mechanisms. The method used to compute the peak positions of the different single and double diffraction beams from the (100) crystal surfaces at normal incidence is described in the Appendix.

B. Difficulties of Assignments Due to
Experimental Uncertainties

It should be emphasized that all of these assignments are tentative and have been made on the basis of the best fit between the calculated and the observed peak positions. Two important parameters have been neglected in arriving at these assignments. The first is inner potential, and the second is that due to experimental inaccuracies.

All of the data which were reported from other laboratories were
obtained via faraday cup detectors.[19,20,21] This published data was
generally accompanied by detailed correlations between the angle at
which a diffraction feature was observed and that calculated from the
plane grating formula using the experimental beam voltage. It may be
seen that in the low eV region (below 50 or 100 eV), as noted by
Farnsworth[19] the agreement is quite good. This agreement between data
and calculations seems to indicate that small inner potential corrections
on the order of 5 eV or less are appropriate in this region. Cursory
studies in this laboratory gave similar results for palladium surfaces.

We have observed that in using the commercial display instruments,
serious discrepancies may exist between the measured electron energy,
and the actual energy of the electrons striking the crystal. This
difference increases with increasing beam voltage and is a function
of the temperature of the cathode. This discrepancy results in an
uncertainty (as much as 5-20 eV) in determining the electron energy
at which diffraction peaks appear. Significant shifts of the I_{hk} vs. eV
curves may occur along the voltage scale as a result of minor changes
in the cathode characteristics. It was not verified if this same effect
exists for the instruments used in the previously published data, but
the good agreement between the calculated and the observed angles would
seem to indicate that at least it could not have been significant
in the low electron energy region.

Another possible source of experimental error was small uncertainties
in the angle of incidence. It was found that slight deviations from
normal incidence resulted in noticeable shifts in peak positions and

changes in peak shape. These variations increased with increasing beam
voltage.

All of these effects tend to make the assignments at the higher
beam voltages less reliable than those at the lower beam voltages.

In order to discuss the properties of the different non-specular
beams separately, and to correlate them to single and double diffraction
events it is useful to arbitrarily divide the electron energy range
in which they were studied into four ranges; I) 0-20 eV, II) 20-40 eV,
III) 40-80 eV and IV) > 80 eV.

C. Beam Voltage Range ~ 0-20 eV

In this region, below the appearance voltage of the first order
diffraction beams, only the specularly reflected beam (00-reflection)
is directly observable. There are only two elastic scattering phenomena
expected in this region. The first is the appearance of a Bragg peak,
$(2 K_z^{\circ} = G_z)$, predicted by both the single (kinematic) and the multiple
scattering theories. The second phenomena is the resonance maximum
predicted solely by the multiple scattering approach and discussed in
detail by McRae.[2a] Just below the beam voltage at which the first order
diffraction beams appear for the (100) face of a simple cubic crystal,
there should be a maximum in the specularly reflected (00) beam. This should
be immediately followed by a resonance minimum in the (00) beam at the
emergence voltage of the (10) beam. This resonance minimum has been
experimentally observed on LiF[9] and is considered to be one of the
experimental verifications of the multiple scattering nature of low energy
electrons (in addition to the presence of double diffraction peaks).

In the experimentally observed specularly reflected (00) beam
intensities from the (100) faces of aluminum and palladium, only one
maximum is observed in this region, at around 10 eV and 15 eV, respectively.
These values are slightly higher than those expected for the appearance
of the Bragg maxima. It should be noted that the quality of the data
is relatively poor in this low voltage region due to the low current
levels of the electron gun. A more detailed investigation in this range
with constant current electron source and using more sensitive detection
techniques would be useful.

D. Beam Voltage Range ~ 20-40 eV

The second region which starts above the appearance voltage of
the first order diffraction (10) beams, but ends just below the
appearance voltage of the second order diffraction beams is more complex
than the first region due to the increase in the number of beams that
are present [(00) and (10)]. At the emergence voltage, a diffraction
condition of the form $\vec{K}_z^{10} - \vec{K}_z^{10} = \vec{G}_z$, is met, where $\vec{G}_z$ is the perpendicular
component of the reciprocal lattice vector with zero magnitude. This,
of course, is the condition for surface wave resonance. This intensity
maximum which should appear in the (10) beam has not been observed in
any of the data reported here, presumably because of experimental limita-
tions. However, Jones[3] has observed high intensity first order diffraction
beams at the emergence voltage.

The second phenomena in this region, which should occur at a slightly
higher beam voltage, is characterized by a diffraction condition of

the form $K_z^{OO} + K_z^{1O} = G_z$. If single scattering predominates, this diffraction process would produce an intensity maximum only in the first order, (10), diffraction beam. Multiple scattering considerations indicate that there should be a maximum in the specularly reflected beam as well.

The available experimental data for the first order diffraction beams from aluminum and palladium do not extend into this low voltage range. However, for silver,[20,21] copper[21] and nickel,[19] intensity maxima are reported in the (10) beams within about 1 eV of the respective calculated values for the single scattering process $(K_z^{OO} + K_z^{1O} = G_z)$. No equivalent peak has been reported for gold, but it may have been outside of the range of experimental observation.[20]

The next predicted maximum involves a diffraction condition of the form $2K_z^{1O} = G_z$. This is strictly a multiple scattering effect as it formally necessitates at least double diffraction. This region is still outside of the experimentally observed range for palladium, but maxima have been observed for aluminum,[14b] nickel,[19] copper,[21] gold[20] and silver[20,21] within 3 eV of the respective calculated theoretical values. The maxima for nickel is distinct but weak in the curves reported by Park[19a] and appears only as a shoulder in the curves reported by Farnsworth.[19b] This is an example of the sensitivity of peak shape and position to slight variations in the experimental arrangement.

This peak is of particular interest for several reasons. First, it is forbidden in the kinematic limit of diffraction and therefore may be taken as evidence of multiple scattering. Secondly, it is the first of a general class of dominant peaks (ignoring surface wave resonance)

that are characterized by the equation, $2\vec{K}_z = \vec{G}_z$. Here the diffraction interaction involves beams differing primarily in the sign, but not the magnitude of that component of their wave vector (or momentum) that is perpendicular to the surface.

At a slightly higher beam voltage, there is predicted, a 1/2-ordered secondary Bragg maximum in the specularly reflected beam. This effect has been discussed by McRae[4b] and is associated with a diffraction condition of the form $\vec{K}_z^{00} - \vec{K}_z^{10} = 1/2\ \vec{G}_z$. In the first order diffracted beams from the (100) face of Au and Ag,[20,21] and possibly from Ni[19c] and Cu,[21] there appear intensity maxima in this voltage region. It should be noted that all of these maxima appear at uniformly higher voltages than those predicted.

The relative intensity of this maxima generally increases with increasing atomic number. That is, it is not observed on aluminum,[14b] is weak or questionable on nickel[19] and copper[21] but is quite prominent for gold and silver.[20,21] This region for palladium was outside of the range of experimental observation. Regardless of the assignment of this diffraction peak, this trend in intensities is a manifestation of the effect of varying the potential at the scattering centers by varying the atomic number.

There are no further maxima in the first order diffraction beams below the emergence voltage of the (11) diffraction beams. All of the preceding phenomena may contribute to the intensity of the specularly reflected beam in this region. Comparisons with experiment are complicated by the fact that the intensities of the specularly reflected beam can not be obtained at normal incidence. Aluminum shows a rather

featureless hump in this region at 0 ~ 3°. Palladium shows a gradual

increase in intensity throughout the region. More structure is observable

on copper[21] where there are two distinct maxima in this region. It is

probable that all of the phenomena contribute to the intensity of the

(00) beam in this range. Careful angular studies should allow one to

distinguish among the various components.

E.   Beam Voltage Range ~ 40-80 eV

This is the region between the appearance of the second order

diffraction beams (11) and the third order diffraction beams (20).

For the (100) face of face centered cubic metals at normal incidence,

the appearance of the (11) beams coincides with the second Bragg maxima

in the specularly reflected beam. McRae[2a] has concluded that there

should be a zero in the reflectivity curve for the h,k beam when the

following two conditions are met simultaneously $K_{h,k} = n2\pi/d$ and

$K_{h',k'} = 0$. In this case, the first condition corresponds to the Bragg

maxima in the (0,0) beam, and the second to the surface wave resonance

in the (11) beams. Consequently, at normal incidence, there should be a

minima in the specularly reflected beam in this region in the fully

elastic multiple scattering model. Such a minima is observed for aluminum,

and possibly for copper.[21] Data for gold, silver and nickel were not

investigated. No such minima is observed in the specular, (00) beam,

for palladium. As all of the data for the specularly reflected beam

was taken at non-normal incidence, it is difficult to conclude anything

about the magnitude of this effect for these materials. It is possible

that the intensity of this diffraction feature becomes more pronounced

with decreasing atomic number.

The first diffraction condition that is met after the appearance
of the (11) beams is between the (11) beams and the (10) beams and is
characterized by a diffraction condition of the form $K_z^{10} + K_z^{11} = G_z$.
This may produce observable maxima in either set of beams. No intensity
maxima have been reported in this region for the (11) beam, possibly
due to the experimental difficulties inherent in investigating a beam
this close to its emergence voltage. The (10) beam represents a different
case however. Here the experimental data is reliable, and an intensity
maxima is definitely observed in this region for both aluminum[14b] and
nickel[19] within 2 eV of the calculated values. In addition, there is a
definite shoulder for silver[21] just below 40 eV (calculated value 38.6 eV).
No maxima have been reported in this region for the (10) beams from
gold[20] and copper,[21] but it is possible that they may be present as a
shoulder or a very weak peak masked by adjacent phenomena. The data
for palladium does not extend into this region.

At higher energies, there are two diffraction conditions that are
met almost simultaneously. The first is of the form $2K_z^{11} = G_z$, and,
approximately one electron volt higher, there is another of the form
$K_z^{00} + K_z^{10} = G_z$. Except perhaps for nickel, there is a uniform absence
of significant intensity maxima in the (10) beams in this range (approximately
45-55 eV for Pd(100)). However, for the (11) beams, definite maxima
are observed for silver,[20,21] copper[21] and nickel within several electron
volts of the positions calculated from $2K_z^{11} = G_z$. Similarly, there
appears to be a shoulder in this region for gold. There is a conspicuous
absence of any strong maxima in this range in the data from palladium.[16]
The curves for aluminum do not extend into this range. This is a region

where intensity maxima in the (10) beams that should be allowed in the

kinematic limit are not observed, possibly being suppressed by a

multiple scattering event involving the (11) beams.

Proceeding to still higher energies, we encounter strong maxima

in the (10) beams diffracted from all of the materials under investigation.

All of the positions are within three electron volts of those calculated

from the diffraction condition $2K_z^{10} = G_z$ and there are no other diffraction

conditions involving this beam within approximately a 10 volt range.

These maxima are generally quite strong and represent one of the more

notable and consistent correlations between materials made in this study.

As these peaks are relatively strong, they tend to dominate a fairly

large energy range. As a result, weaker peaks may be obscured making

interpretation in adjacent regions somewhat difficult.

On the high energy side of these intensity maxima in the (10) beam

there is some indication of a shoulder for several materials, and definite

maxima for both gold[20] and silver.[20,21] The higher peaks on silver and

gold are within five and three electron volts respectively of the positions

calculated for a half order Bragg peak in the specularly reflected

beam that would involve a diffraction interaction between the (00) and the

(10) beams. However, they are within three and one electron volts,

respectively, of the positions calculated for the diffraction condition

$K_z^{10} + K_z^{11} = G_z$. There are no corresponding peaks reported in the (11)

beams for any of the materials observed in this range.

At slightly lower energies (62.5 eV for palladium) there are definite

intensity maxima in the (11) beams for all of the materials investigated

in this region. Furthermore, all of these maxima are within one eV

of the positions calculated from the diffraction condition $K_z^{OO} + K_z^{11} = G_z$, with the exception of that for silver[21] which is within three eV of the calculated position. These maxima presumably are a manifestation of a diffraction condition that is allowed in the limit of kinematic scattering.

F.   Beam Voltage Range > 80 eV

The next diffraction process of interest is the appearance of the (2,0) diffraction beams and approximately 20 eV higher, the (2,1) beams. It becomes excessively tedious to enumerate in detail all of the possible diffraction conditions as the number of possible types of interaction increases rapidly with the number of beams present even at normal incidence. Away from normal incidence, the situation should be considerably more complicated. Furthermore, as the band structure becomes more complex, bands overlap and the interpretation becomes more difficult. Fewer of the diffraction conditions are met "purely", i.e., without any mixing and not all of the allowed conditions will be observed as multiple scattering may become less pronounced. Comparisons with experimental data also become less reliable at higher beam voltages unless extreme care was exercised in obtaining that data. In general, however, the analysis can be carried out in the same manner as above. The results of such an analysis are tabulated in Table II. There are several points of interest. At normal incidence, the appearance of the (2,0) beams coincides exactly with a diffraction condition of the form $2K_z^{11} = G_z$ for the (1,1) beam. Therefore, a diffraction condition of the form $K_z^{11} - K_z^{2O} = G_z$ is automatically met. Accordingly, there should be a

resonance minima in the back reflected (1,1) beam intensity.[2a] In fact,
no strong maxima are observed or reported for the (1,1) beams in this
region for any of the materials under consideration. This may be taken
as an indication of the significance of the resonance effect in this
region for these materials. It should be noted that there are very
weak maxima observed in this general region for the (1,1) beams of
several of these materials.[19,20,21] However, on palladium it has been
noted that this beam is very sensitive to position and that its appearance
is probably due to small deviations from perfectly normal incidence.

As with the n = 2 Bragg peak, there is a similar coincidence for
the n = 4 Bragg peak. In fact, it may be shown that all of the even
integral order Bragg peaks from the (100) face of fcc materials at
$\theta = 0°$ coincide with the appearance of some set of (h,h) beams. Consequently,
there should be a resonance minima rather than a Bragg maxima at these
voltages in the fully elastic multiple scattering treatment developed
by McRae.[2a] On Al, Pd, Pt,[15] and Cu[21], a minimum is observed in the
specular reflected beam at the appropriate voltage. However, on all of
these materials, a strong maxima is observed approximately 20 eV lower.
It is tempting to assign this to a Bragg peak with a reasonable inner
potential and say that the resonance minima is not observed. The former
may be correct, but the latter is not necessarily so as all the observations
were carried out at $\theta = 0°$. McRae[2a] has shown that for slight deviations
from normal incidence, the Bragg peak may appear and that its shape
structure may still be strongly influenced by the coupling with the
surface wave resonance that accompany the emergence of the new
diffraction beams.

There is another interesting feature in this region that may be associated with simultaneous diffraction conditions. On aluminum, very strong intensity maxima in the (1,0) beam occurs at approximately 100 eV. There are at least four diffraction conditions which may be met; $2K^{10} = G_z$, $K_z^{10} + K_z^{21} = G_z$, $2K_z^{21} = G_z$ and $K_z^{10} - K_z^{21} = G_z$. On the high energy side of this maxima for aluminum, a definite shoulder is observable. Going to the corresponding region on nickel,[19a,19b] one finds that the relative intensity of the shoulder is comparable to that of the main beam. Continuing to the noble metals, it may be seen that the peak that was so intense for aluminum has essentially vanished, and that the region is dominated by what was the shoulder. It would be interesting to investigate the behavior of the (2,1) beams in this range in order to observe whether or not they manifest the inverse trend in intensities. If so, this would provide an interesting correlation between scattering amplitudes and potentials for the different metals.

Conclusion

The properties of the non-specular low energy electron beams seem to verify the importance of multiple scattering in low energy electron diffraction. This is consistent with earlier observations on the specularly reflected beam.[9] The number of observed diffraction maxima is too large to allow for their assignment solely on the basis of kinematic considerations. The coincidence of observed intensity maxima positions with those calculated on the basis of a double diffraction mechanism would seem to substantiate the validity of the double diffraction approach[4b] in predicting possible peak positions [though not their intensities]

The double diffraction condition, $2K_z' = \vec{G}_z$ appears to be particularly

dominant in the electron energy just above the appearance energy of the

beam under consideration. There also appears to be a general tendency

for diffraction conditions with relatively small magnitudes of $\vec{G}$ to

dominate. As most atomic potentials would favor forward scattering

this is physically reasonable.[22]

Assuming that the preceding assignments are at least partially correct,

inner potential corrections appear to be considerably less than 10 eV

and probably less than 5 eV in the very low energy range. This would

be in agreement with the earlier angular studies by Farnsworth.[21]

Finally, it may be seen that the atomic potential plays a significant

role in determining peak shape and intensity.

References

1. C. Davisson and L. H. Germer, Proc. Nat. Acad., 14, 619 (1928).

2a. E. G. McRae, J. Chem. Phys., 45(9), 3258 (1966).

2b. E. G. McRae, Surf. Sci., 8, 14 (1967).

3. D. S. Boudreaux and V. Heine, Surf. Sci, 8, 426 (1967).

4a. E. G. McRae, Surf. Sci., 11, 479 (1968).

4b. E. G. McRae, Surf. Sci., 11, 492 (1968).

5a. K. Kambe, Z. Naturforsch., 22A, 322 (1967).

5b. K. Kambe, Z. Naturforsch., 22A, 422 (1967).

6. K. Kambe, Z. Naturforsch., 23A, 1280 (1968).

7. G. Gafner, Calculation of Back-Reflected Leed Intensities Using a
Plane Wave Multiple Scattering Mechanism in the Structure and
Chemistry of Solid Surfaces, G. A. Somorjai, ed., Proceedings of
the Fourth International Materials Symposium, Berkeley, 1968.

8. P. M. Marcus and D. W. Jepsen, Phys. Rev. Letters, 20, 925 (1968).

9. E. G. McRae, Surf. Sci., 7, 41 (1967).

10a. P. J. Estrup and J. Anderson, Surf. Sci., 8, 101 (1967).

10b. N. J. Taylor, Surf. Sci., 4, 161 (1966).

11. Varian, Low Energy Electron Diffraction System, Model No. 981-0000,
611 Hansen Way, Palo Alto, California, U.S.A.

12. Philips Metalonics, Impregnated Cathode, Type B, 88 S. Columbus
Avenue, Mt. Vernon, New York.

13. Materials Research Corporation, Post Office Box 14, Redwood City,
California.

14a. F. Jona, J. Phys. Chem. Solids, 28, 2155 (1967).

14b. S. M. Bedair, F. Hofmann and H. P. Smith, J. Appl. Phys., 39(8), 4026
(1968).

15. R. M. Goodman, H. H. Farrell and G. A. Somorjai, J. Chem. Phys., $\underline{49}$(2), 692 (1968).

16. R. L. Park and H. H. Madden, Jr., Surf. Sci., $\underline{11}$(2), 188 (1968).

17. R. M. Goodman, H. H. Farrell and G. A. Somorjai, J. Chem. Phys., $\underline{48}$(3), 1046 (1968).

18. E. R. Jones, J. T. McKinney and M. B. Webb, Phys. Rev., $\underline{151}$(2), 476 (1966).

19a. R. L. Park, J. Appl. Phys., $\underline{37}$(1), 295 (1966).

19b. H. E. Farnsworth, et al., J. Appl. Phys., $\underline{29}$(8), 1150 (1958).

19c. M. Onchi and H. E. Farnsworth, Surf. Sci., $\underline{11}$(2), 203 (1968).

20. H. E. Farnsworth, Phys. Rev., $\underline{43}$, 900 (1933).

21. H. E. Farnsworth, Phys. Rev., $\underline{40}$, 684 (1932).

22. This generalization, of course, is not meant to preclude oscillatory behavior in the form factors with increasing values of $|\vec{G}|$.

Appendix

The wave vector of the incident electron beam may be expressed in a Cartesian Coordinate System as

$$\vec{K}^\circ = \vec{K}_x + \vec{K}_y + \vec{K}_z \quad . \tag{7}$$

Defining Θ as the angle of incidence with respect to the surface normal and φ as the azimuthal angle we have

$$|\vec{K}_x| = |\vec{K}^\circ| \sin \Theta \sin \varphi \tag{8a}$$

$$|\vec{K}_y| = |\vec{K}^\circ| \sin \Theta \cos \varphi \tag{8b}$$

$$|\vec{K}_z| = |\vec{K}^\circ| \cos \Theta \quad . \tag{8c}$$

Using Equation (4) and Equations (8a) and (8b), the x and y components of the wave vector characterizing a diffracted beam can be written as

$$|\vec{K}_x'| = |\vec{K}^\circ| \sin \Theta \sin \varphi + |\vec{G}_x'| \tag{9a}$$

$$|\vec{K}_y'| = |\vec{K}^\circ| \sin \Theta \cos \varphi + |\vec{G}_y'| \quad . \tag{9b}$$

Substituting Equations (9a) and (9b) into Equation (6), we obtain

$$|\vec{K}_z'| = \pm \{ |\vec{K}^\circ|^2 - (|\vec{K}^\circ| \sin \Theta \sin \varphi + |\vec{G}_x'|)^2 - (|\vec{K}^\circ| \sin \Theta \cos \varphi + |\vec{G}_y'|)^2 \}^{1/2} \tag{10}$$

for the component of the diffracted wave vector that is perpendicular to the surface. At normal incidence, $\Theta = 0°$ Equation (10) becomes

$$|\vec{K}'|_z = \pm \{ |\vec{K}^\circ|^2 - |\vec{G}_x'|^2 - |\vec{G}_y'|^2 \}^{1/2} \tag{11}$$

Substituting Equation (11) into the diffraction equation, Equation (5), we have

$$\pm \{|\vec{K}^\circ|^2 - |\vec{G_x'}|^2 - |\vec{G_y'}|^2\}^{1/2} \mp \{|\vec{K}^\circ|^2 - |\vec{G_x''}|^2 - |\vec{G_y''}|^2\}^{1/2} = |\vec{G_z}| \quad (12)$$

where the appropriate signs are taken for the situation under consideration. Noting that

$$|\vec{K}^\circ| = 2\pi \{eV/150.4\}^{1/2} \; ; \quad |\vec{G_x}| = 2\pi h/a_x \; ; \quad |\vec{G_y}| = 2\pi k/a_y$$

and $|\vec{G_z}| = 2\pi n_z/a_z$, Equation (12) may be written as

$$\pm \{\frac{eV}{150.4} - (\frac{h'}{a_x})^2 - (\frac{k'}{a_y})^2\}^{1/2} \mp \{\frac{eV}{150.4} - (\frac{h''}{a_x})^2 - (\frac{k''}{a_y})^2\}^{1/2} = \frac{n_z}{a_z} \quad (13)$$

where $\vec{a}_x$ and $\vec{a}_y$ are the primitive translations in the two dimensional lattice net parallel to the surface, and $|\vec{a}_z|$ is the distance between planes that are parallel to the surface. For the (100) face of face centered cubic materials, $|\vec{a}_x| = |\vec{a}_y| = \frac{a_o}{\sqrt{2}}$ and $|\vec{a}_z| = \frac{a_o}{2}$ where a_o is the characteristic dimension of the x-ray unit cell (e.g., 4.04 A° for aluminum). Therefore, for the metals reported on here, Equation (13) becomes

$$\pm \{\frac{eV}{150.4} - \frac{2}{a_o^2}[(h')^2 + (k')^2]\}^{1/2} \mp \{\frac{eV}{150.4} - \frac{2}{a_o^2}[(h'')^2 + (k'')^2]\}^{1/2} = \frac{2n_z}{a_o} \quad (14)$$

This equation may be solved analytically, numerically or graphically to determine at what electron energy (in eV) the n_z diffraction condition between the (h', k') beam and the (h'', k'') beam is met.

Table I

Experimentally observed positions (in electron volts) of intensity maxima in non-specularly diffracted beams for the (100) faces of several face centered cubic crystals at normal incidence.

First Order (01) Diffraction Beams

Al[a] (100) (eV)	Pd[a] (100) (eV)	Ag[b] (100) (eV)	Au[c] (100) (eV)	Cu[d] (100) (eV)	Ni[e] (100) (eV)
59	57	20	27.5	26.5	29
72	78	27	32.0	37.3	35
110	98	34.0	55.0	69.7	47
135	120	56.0	64.0	87.0	55
170	141	62.0	117.0	127.5	62
180	173	115.0		146.0	70
29[f]	203	168.3		220.0	92
40[f]		175.5		243.0	132
					145
					187

Table I continued

Second Order (11) Diffraction Beams

Al[a] (100) (eV)	Pd[a] (100) (eV)	Ag[b] (100) (eV)	Au[c] (100) (eV)	Cu[d] (100) (eV)	Ni[h] (100) (eV)
60	81	46.1	58.0	60.3	65
88	106	55	101.5	72.5	78
118	150	75.7	136.0	115.5	100
150	202	93.5	247.0	128.5	120
190	235	141.0		191.5	153
237	625[g]	229.5		210.5	190
		335.5		296.5	
				310.5	

Table I continued

Third Order (02) Diffraction Beams

Al[a] (100) (eV)	Pd[a] (100) (eV)	Ag[b] (100) (eV)	Au[c] (100) (eV)	Cu[d] (100) (eV)
130	174	77.5	70.0	99.0
168	215	112.5	78.5	111.0
200		158.5	120.0	138.0
		173.5	163.0	154.5
		250.5	256.0	203.0
				215.0
				320.0

Fifth Order (22) Diffraction Beams

Ag[b] (100) (eV)	Au[c] (100) (eV)	Cu[d] (100) (eV)
152.5	171.0	200.5
206.5	191.0	260.5
280.5	303.0	277.0

Table I continued

(a) This laboratory average of several runs.

(b) Reference 20 and Reference 21.

(c) Reference 20.

(d) Reference 21.

(e) References 19a, 19b and 19c - averaged.

(f) Reference 14b.

(g) Reference 16.

(h) Reference 19a.

Calculated and Observed Positions of Intensity Maxima
From the (100) Face of Several Face Centered Cubic Metals

Table IIa

First Order (01) Diffraction Beams

h_x k_y h'_x k'_y n_z	Al(100) Calc. (eV)	Obs.[a]	Pd(100) Calc. (eV)	Obs.[a]	Ag(100) Calc. (eV)	Obs.[b]	Au(100) Calc. (eV)	Obs.[c]	Cu(100) Calc. (eV)	Obs.[d]	Ni(100) Calc. (eV)	Obs.[e]
0 1 0 1 0	18.4		20.0		18.1		18.1		23.0		24.3	
0 0 0 1 1	21		23		21	20	21		26	26.5	28	29
0 1 0 1 1	28	29[f]	30		28	27	28	27.5	35	37.3	37	35
						34		32				47
0 1 1 1 1	39	40[f]	43		39		39		49		52	55
0 0 0 1 2	47		51		46		46		58		61	62
0 1 0 1 2	56	59	60	57	54	56	54	55	69	69.7	73	70
0 1 1 1 2	66		71		64	62	64	64	81		86	
		72		78						87		92
0 1 0 2 1	76		82		74		74		95		101	
0 1 0 2 2	88		96		87		87		110		116	
				98								
0 0 0 1 3	94		101		91		91		115		121	

Table IIa continued

h_x k_y h'_x k'_y n_z	Al(100) Calc. (eV)	Obs.[a]	Pd(100) Calc. (eV)	Obs.[a]	Ag(100) Calc. (eV)	Obs.[b]	Au(100) Calc. (eV)	Obs.[c]	Cu(100) Calc. (eV)	Obs.[d]	Ni(100) Calc. (eV)	Obs.[e]
0 1 1 2 1												
0 1 1 2 2	102		110		100		100		127	127.5	133	132
0 1 0 1 3												
0 1 1 1 3	112	110	121	120	109		109		138		146	145
		115				115		117		146		
0 1 0 2 3	132	135	143	141	128		128		165		173	
0 1 2 1 3	143		155		140		140		179		188	187

(a) This laboratory average of several runs.

(b) Reference 20 and Reference 21.

(c) Reference 20.

(d) Reference 21.

(e) References 19a, 19b and 19c - averaged.

(f) Reference 14b.

(g) Reference 16.

(h) Reference 19a.

Table IIb

Second Order (11) Diffraction Beams

h_x k_y h'_x k'_y n_z	Al(100) Calc. (eV)	Obs.[a]	Pd(100) Calc. (eV)	Obs.[a]	Ag(100) Calc. (eV)	Obs.[b]	Au(100) Calc. (eV)	Obs.[c]	Cu(100) Calc. (eV)	Obs.[d]	Ni(100) Calc. (eV)	Obs.[h]
1 1 1 1 0 } 0 0 1 1 ±1 }	37		40		36		36		46		48	
0 1 1 1 1	39		43		39		39		49		52	
1 1 1 1 1	46		50		46	46.1	46		58	60.3	61	65
0 0 1 1 2	58		63	62.5[g]	57	55	57	58.0	72	72.5	76	78
0 1 1 1 2	66		71		64		64		81		86	
1 1 1 1 2 } 1 1 0 2 ±1 }	74		80	81	72	75.7	72		92		97	100
1 1 1 2 -1 } 1 1 0 2 2 } 1 1 2 1 +1 }	94	88	103	106	92	93.5	92		118	115.5	125	120

Table IIb continued

h_x k_y h'_x k'_y n_z	Al(100) Calc. (eV)	Obs.[a]	Pd(100) Calc. (eV)	Obs.[a]	Ag(100) Calc. (eV)	Obs.[b]	Au(100) Calc. (eV)	Obs.[c]	Cu(100) Calc. (eV)	Obs.[d]	Ni(100) Calc. (eV)	Obs.[h]
0 0 1 1 3	104		112		101		101	101.5	128	128.5	135	
1 1 1 2 2	107		116		105		105		133		140	
0 1 1 1 3	112		121		109		109		138		146	
1 1 1 1 3	121	118	130		118		118		150		157	153
1 1 0 2 3	141		152	150	137	141	137	136.0	180		188	190

(a) This laboratory average of several runs.

(b) Reference 20 and Reference 21.

(c) Reference 20.

(d) Reference 21.

(e) Reference 19a, 19b and 19c - averaged.

(f) Reference 14b.

(g) Reference 16.

(h) Reference 19a.

Table IIc

Third Order (02) Diffraction Beams

h_x	k_y	h'_x	k'_y	n_z	Al(100) Calc. (eV)	Obs.[a]	Ag(100) Calc. (eV)	Obs.[b]	Au(100) Calc. (eV)	Obs.[c]	Cu(100) Calc. (eV)	Obs.[d]
0	2	0	2	0								
1	1	0	2	±1	73		72		72	70.0	92	
0	1	0	2	-1	76		74		74		95	
								77		78.5		99
0	2	0	2	1								
0	0	0	2	-1	82		81		81		104	
0	0	0	2	2								
0	1	0	2	2	88		87		87		110	111.0
1	1	0	2	2								
1	2	0	2	1	95		93		93		118	
0	2	0	2	2	111		109	112	109		138	138

Table IIc continued

h_x	k_y	h'_x	k'_y	n_z	Al(100) Calc. Obs.[a] (eV)		Ag(100) Calc. Obs.[b] (eV)		Au(100) Calc. Obs.[c] (eV)		Cu(100) Calc. Obs.[d] (eV)	
1	2	0	2	2	121		118		118		150	
0	0	0	2	3	125		121		121	120	155	154.5
0	1	0	2	3	132	130	128		128		165	
1	1	0	2	3	141		137		137		176	

(a) This laboratory average of several runs.

(b) Reference 20 and Reference 21.

(c) Reference 20.

(d) Reference 21.

(e) Reference 19a, 19b and 19c - averaged.

(f) Reference 14b.

(g) Reference 16.

(h) Reference 19a.
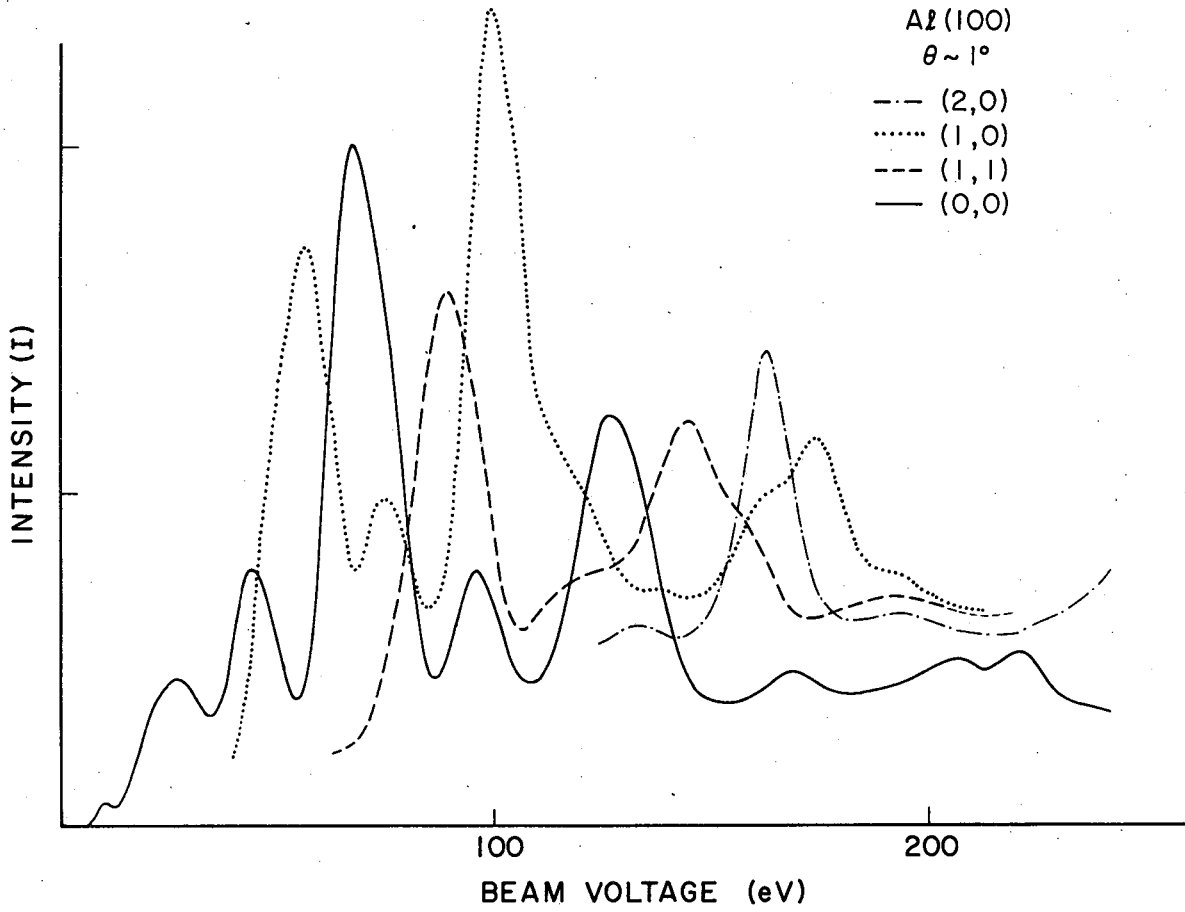
Figure 1. The intensities of several diffraction beams from the Al(100) surface

as a function of electron energy.
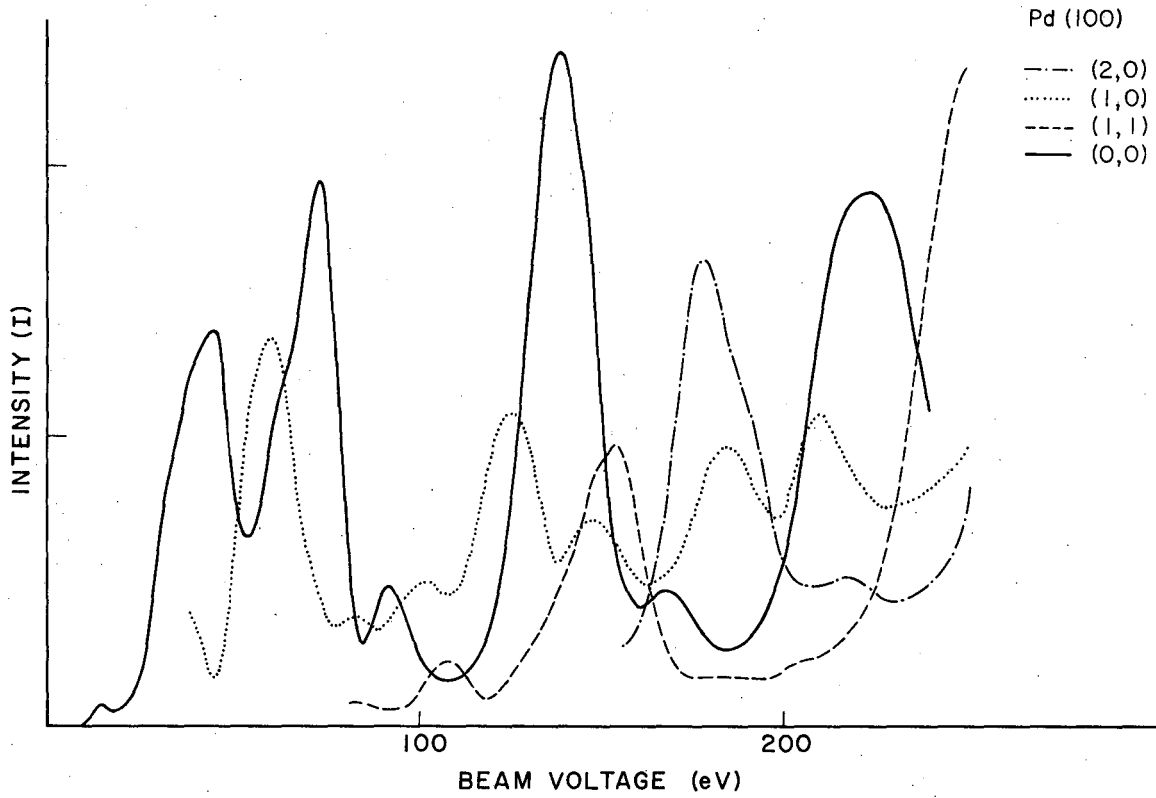
Figure 2. The intensities of several diffraction beams from the Pd(100)

surface as a function of electron energy.

[graphic: schematic diffraction pattern]

● [01]   ● [11]

● [00]   ● [10]   ● [20]
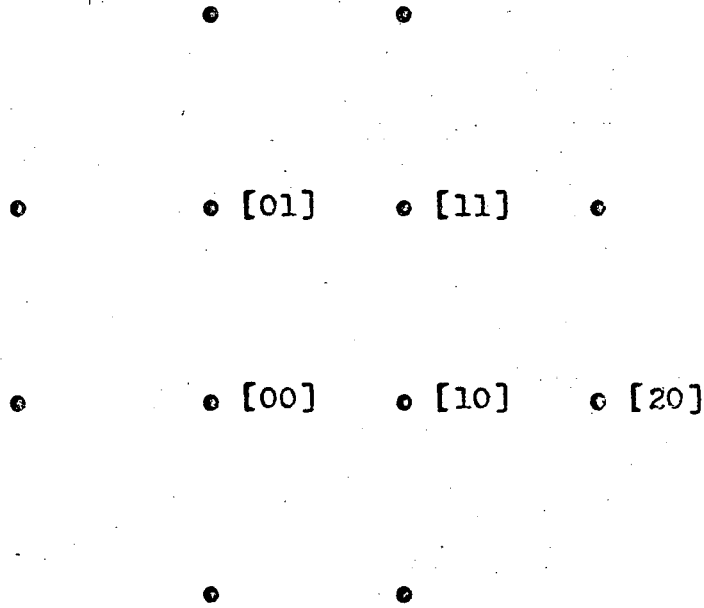
Figure 3.   Schematic diffraction pattern from the (100) surface of

f.c.c. solids indicating the assignments used to identify

the diffraction beams.

Figures 4a and 4b. The intensities of the a) (10) and b (11) diffraction

beams as a function of normalized electron energy

for the (100) face of aluminum, copper, nickel,

palladium, silver and gold.

$\theta = 0°$

Al

Cu

Ni

Pd

Ag

Intensity (I_{10})

1200   2400   3600

$eV \, d^2 \cos^2\theta$

Figure 4a.

Figure 4b.